GRASSLAND SCIENCE

Japanese Society of Grassland Science

Japanese Society of Grassland Science ISSN1744-6961

ORIGINAL ARTICLE

Mapping the spatial distribution of soil depth in a grassland ecosystem with the aid of ground penetrating radar and GIS (Northwestern Sichuan, China)

Xuelian Zhang[1,2], Ligang Dao[3], Chaosheng Zhang[4], Liam Morrison[5], Bing Hong[6], Hongxuan Zhang[3] and Youmin Gan[1]

1 Sichuan Agricultural University, Chengdu, China
2 Management Center of Education Infrastructure Equipment and Asset, Minhang District, China
3 GIS Centre, Sichuan Academy of Grassland Science, Chengdu, China
4 School of Geography and Archaeology, National University of Ireland, Galway, Ireland
5 Earth and Ocean Sciences, School of Natural Sciences and Ryan Institute, National University of Ireland, Galway, Ireland
6 State Key Laboratory of Environmental Geochemistry, Institute of Geochemistry, Chinese Academy of Sciences, Guiyang, China

Keywords
GIS; ground penetrating radar; soil depth; spatial distribution.

Correspondence
Youmin Gan, Sichuan Agricultural University, Chengdu, 611130 Sichuan, China.
Email: ganyoumin1954@163.com

Received 9 September 2016; accepted 8 January 2018.

doi: 10.1111/grs.12201

Abstract

Obtaining accurate soil depth information is critical to improving how we assess the health and manage of soil resources that contribute to sustainable management of agricultural lands. While there are many techniques to assess soil characteristics, using ground penetrating radar (GPR) to determine soil depth has received little attention. This study aimed to determine the suitability of GPR for obtaining accurate soil depth information over a 10 km intervals grid system in a generally flat grasslands ecosystem in the Sichuan Province of China. Geographic information system (GIS) and geostatistical techniques were used to map the spatial distribution of soil depth across the field site. Images created from GPR were filtered using DC removal and automatic gain control, and log-transformation was used to transform the raw data in order to conform a normal distribution. The soil depth data were spatially interpolated across the field site using the geostatistical techniques of (semi-) variogram and ordinary kriging (OK), then ground-truthed and validated via comparison with traditional methods and previously collected data. A total of 39 random data points (ruler-measured and GPR data) were selected to evaluate the accuracy of the GPR, and results showed that the difference were within 3 cm of the actual soil depth in 93% of all samples, and within 5 cm in all samples ($R^2 = 0.914$). Results confirmed that this GPR reflection technique has the potential to precisely and quickly measure soil depth over large areas and under variable topography, contributing to the body of technical information that can help inform soil management policy for sustainable agriculture. The spatial distribution map of soil depth produced with the aid of OK demonstrated the accuracy and non-destructive features of GPR, which is able to provide a more detailed map of soil depth than methods used in previous grassland soil depth studies.

Introduction

Soil depth, also called "regolith depth" (Craig 1978; Cerdà and García-Fayos 1997) or "soil thickness" (Kuriakose *et al.* 2009), refers to the vertical depth of soil from the surface to the consolidated material where plant roots are distributed (Kuriakose *et al.* 2009). This is a primary indicator of soil quality, and exerts significant influence on vegetation yield (Fuhlendorf and Smeins 1998; Meyer *et al.* 2007). A decrease in soil depth may result in reduced vegetative productivity (Rhoton and Lindbo 1997), landslides and soil erosion (Bathurst *et al.* 2007), and water loss (Wang *et al.* 2006). To better understand and more sustainably manage soil resources, detailed soil depth information is critical.

Direct measurements of soil depth can be difficult to obtain over large areas with diverse topography, and are influenced by local micro-topography, parent material and hydrogeological conditions (Moore *et al.* 1993; Dietrich *et al.* 1995; Johnson *et al.* 2005). Adding to the complexity of obtaining accurate measurements, these variables can be mutually interactive. Soil depth varies according to local topography (Lee *et al.* 1988; Gessler *et al.* 2000; Pachepsky *et al.* 2001), water retention (Whelan *et al.* 2005), vegetative cover (Meyer *et al.* 2007), and geological features (Minasny and McBratney 1999). Conventional soil depth measurement techniques include invasive methods such as coring and test pit excavations (Phillips 2010), which are often time consuming, expensive, damage the soil, and only provide point-specific information. Previous studies have attempted to determine soil depth by using electrical resistive imaging combined with conventional invasive methods, and have failed to clearly identify how the sub-surface properties are spatially distributed (Yamakawa *et al.* 2012). Other studies have predicted soil depth by building models based on discrete element methods using measured variables such as slope, curvature and profile curvature, wetness index, land use, distance from streams and platform curvature (Cundall and Strack 1979; Pennock and De Jong 1987; Lin and Ng 1997; Chareyre and Villard 2005; Güneralp and Rhoads 2009). Although less time consuming, these models involve dividing each soil site into a number of interconnected discrete elements and are limited by the complexity of the topography of the study area. Model accuracy is also affected by the presence of gentle convex undulations and undifferentiated surfaces in the topography, which cannot be unequivocally discriminated from each other in a digital elevation model (DEM) (Chartin *et al.* 2011).

More recently, ground penetrating radar (GPR) has been successfully used to quantify spatial distribution soil water and moisture content (Chanzy *et al.* 1996; Hubbard *et al.* 2002; Schmalz and Lennartz 2002; Grote *et al.* 2003; Huisman *et al.* 2003; Galagedara *et al.* 2005; Minet *et al.* 2010; Sucre *et al.* 2011), soil roughness (Lambot *et al.* 2006), snowpack thickness (Previati *et al.* 2011), and organic matter thickness (Shih and Doolittle 1984). However, GPR has not yet been used to investigate and determine soil depth in grassland ecosystems. The applications of GPR across soil and environmental science have shown that this technology is significantly less time consuming, and can provide a continuous characterization of the soil structure compared with conventional coring and test pit excavation methods (Davis and Annan 1989; Gerber *et al.* 2010). In this study, GPR was used to determine soil depth in a grassland ecosystem of the Qinghai Tibet Plateau.

The primary industry in this region is livestock husbandry, and the lack of suitable forage causes a substantial loss of livestock on an annual basis. According to previous studies, from the 1950s to 2000s, total biomass in the grassland decreased approximately 50% (Kreutzmann 2012). To promote the sustainable development and management of grassland ecosystems, pasture development (Prior 1994) and rangeland management program was initiated in the 1990s (Sandford 1983; Moris 1988) that concentrated on both reducing overgrazing and simultaneously aiding socio-economic development in the agricultural sector. These policies were aimed at developing appropriate pastures on flat, accessible areas with deep soils rich in organic matter. To help create these management policies, a National Grassland Survey carried out in during the 1980s at a topographic maps-scale of 1: 200 000 with one sample taken per 10000 ha (Qin *et al.* 1984) collected data in this area measuring soil nutritional elements, soil organic matter, vegetation cover, and biomass. In the same study, the soil depth at 164 sites was measured using coring and test pit excavation methods (Qin *et al.* 1984). However, the spatial distribution of soils has seldom been a factor considered in policies that attempted to help establish sustainable pastures and grasslands.

This study investigated the suitability of GPR for measuring accurate soil depth in a grassland ecosystem in a northwest Sichuan Province in the Qinghai Tibet Plateau, China. Additional GIS and geostatistical techniques were added to continuously interpolate and map the spatial distribution of soil depth across the field site to assist in the development of sustainable pastures and healthy grassland ecosystems at a fine scale. To test the accuracy of the method, the ruler-measurement data were compared and the past data in the 1980s (Qin *et al.* 1984) were used to verify the distribution map.

Materials and methods

Study area and soil investigations

With a total area of approximately 8400 km^2, the grassland under study is in Hongyuan County (Sichuan Province), in the southeast Qinghai Tibet Plateau (Himalayan Plateau) approximately 3500 m above sea-level [NW (33°05′N, 103°21′E), NE (33°18′N, 102°47′E), SW (31°51′N, 102°39′E), and SE (32°17′N, 101°03′E)]. The climate is influenced by the summer monsoon from the Indian Ocean (Yamamoto *et al.* 2010), and receives approximately 750 mm of average annual precipitation (Hong *et al.* 2003). Sampling locations (n = 121) were determined based on a grid system of 10 km intervals and were generally flat (slope angle < 12°), which allowed easier access (Figure 1). The ruler-measurements were simultaneously carried out at random in 39 places and used to test the accuracy of GPR. Field sampling was conducted between July and October 2012 on dry days (defined as at least 2 days after any rainfall event).

Ground penetrating radar measurements

The GPR system (MALA ProEx, 500 MHz, MALÅ Geosciences, Sweden) consisted of a pulse transmitter antenna, a receiver antenna, and a control unit, which provided high-resolution images of subsurface features in the form of a profile view (Figure 2). The pulses of electromagnetic energy emitted through the soil have distinct characteristics, which can contact a boundary layer or an abnormality (i.e., soil, parent material). The image is the electromagnetic equivalent of a single-trace acoustic profiling system, which is essentially an image of the variation in ground permittivity (Lowe 1985; Daniels 2004). Using the equation below to calculate the velocity of pulse propagation (Daniels 2004)

$$V = 2D/T,$$

which describes the relationship between the propagation velocity (V), depth (D), and two-way pulse travel time (T). Before the GPR was used, a metal calibration plate was buried at a known depth (50 cm in the study) to estimate the velocity of propagation (0.1 m ns^{-1}) and determine the depth of soil. In the study, travel time of the two-way radar pulse and the propagation velocity were compared to show the situation of subsurface interfaces and calculate the soil depth.

Data analyses

GPR signal processing and analysis

To facilitate the extraction of soil depth information from the raw GPR signal, standard signal processing techniques were used. Using data acquisition software (Ground Vision v.2.1, MALA Geosciences, Skolgatan, Sweden), images were filtered by zero drift removal (DC removal), amplification of deep signals (automatic gain control), dislodging of direct wave and other horizontal and inherent signals (subtract mean trace), and removal of unnecessary low-frequency and high-frequency ingredients (band pass) (detailed process described in Neal (2004)).

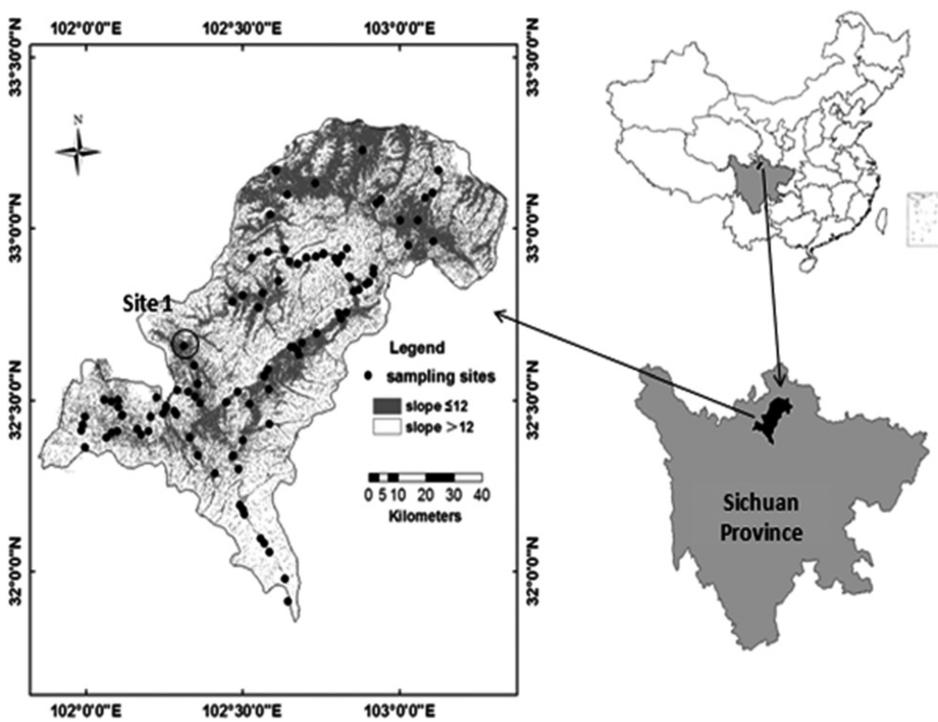

Figure 1 Map showing soil sampling locations in Hongyuan, Sichuan, China (shadowed areas with slope 12°).

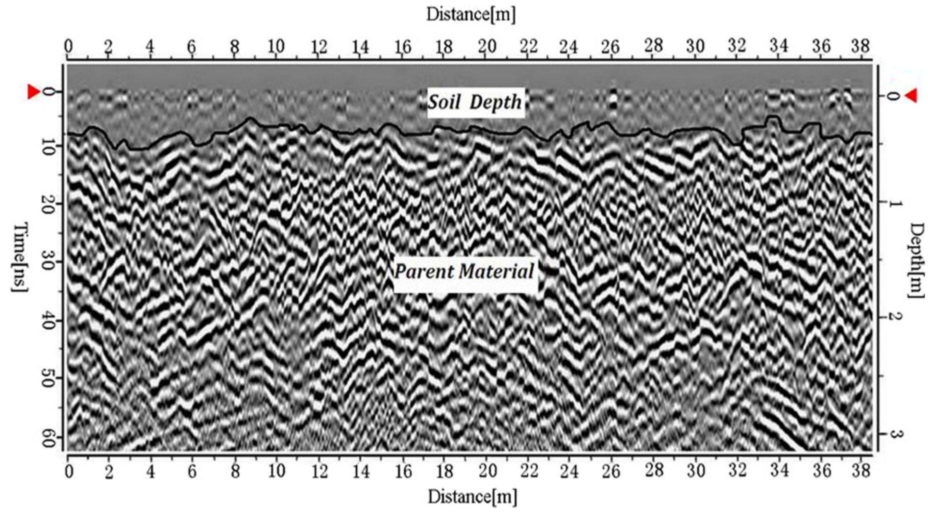

Figure 2 Ground penetrating radar (GPR) reflection record in sampling site 1 soil depth value was calculated per meter (showing soil depth and parent material within 38 m).

Through these signal processing techniques, the flooding waves were removed while the signal intensity of useful waves was retained, which facilitates the extraction of soil depth information from the signal with the aid of the equation.

Probability distribution

Before the production of the spatial distribution map of soil depth, the data were tested to establish whether they conformed to a normal distribution. Any violation of normality, such as high skewness or outliers, can impair the variogram structure and kriging results (Helsel 1987; McGrath and Zhang 2003). Soil depth data were transformed and normalized using a log-transform, a commonly used transformation method in soil science (Beaver *et al.* 1985) and was used to normalize the data set in this study (with a Kolmogorov–Smirnovtest P-value of 0.093).

Spatial structure

To create a spatial distribution map of soil depth, ordinary kriging (OK) was used to interpolate available and collected data across the field site. Spatial variability was modeled using a (semi-) variogram, and appropriate input parameters were identified for the spatial interpolation (McBratney and Webster 1986; Oliver and Webster 1986) using Variowin 2.2 software (Weijun *et al.* 2010). A series model's parameters (Range, Sill, Partial Sill and Nugget) were calculated to select the appropriate (semi-) variogram models, the minimal measuring error (Nugget) model was selected as the optimal model used in the study.

Results

GPR Performance

Several nature profiles were chosen to evaluate the accuracy of GPR, 39 sites were chosen randomly by ruler-measurements and GPR simultaneously. A scatter plot (Figure 3) shows the comparison of the ruler-measured versus GPR data, which showed that most data were located closely along a diagonal line, indicating that GPR is reliable when measuring soil depth in this area. However, a few observed outliers that require further investigation may be attributed to sampling errors, measurement errors, or the process of extracting readings from the GPR images. The difference between ruler-measured data and GPR-detected data were within 3 cm for 93% of samples, and within 5 cm in all samples. Other studies have also found GPR to have a reliable performance when measuring soil depth. For example, in the Florida Everglades' Agricultural Area, GPR was used to determine the thickness of the organic soil layer, and showed a similarly relatively high correlation coefficient of 0.84 between the ruler-measured depth and the GPR-detected depth (Shih and Doolittle 1984).

Basic statistics

Across the 121 GPR-created images and sampling sites soil depth data, basic statistics including the minimum, 25th percentile, median, 75th percentile, 95th percentile, maximum, mean, skewness, kurtosis and standard deviation were calculated (Table 1). Approximately 75% of the

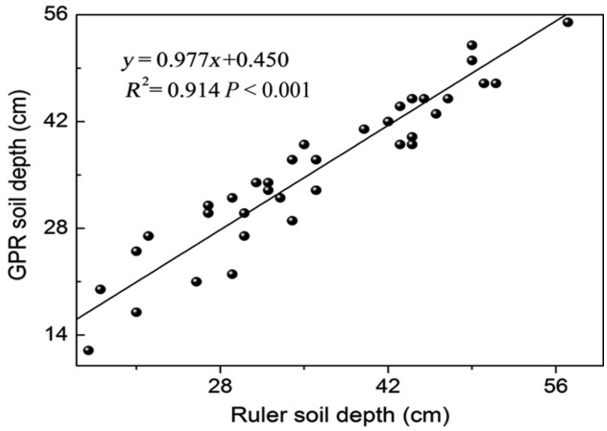

Figure 3 A comparisons between soil depth values (per point) measured by ground penetrating radar (GPR) and ruler (n = 39, R^2 = 0.914).

sampling values were less than 57 cm. The large differences between the minimum and maximum value and high standard deviation revealed the heterogeneous nature of soil depth in the study area. Meanwhile, the high skewness and kurtosis values indicated the raw data set was not normally distributed, which necessitated the log-transformation detailed above.

Spatial structure of soil depth

Before selecting the appropriate semi-variogram models for the kriging interpolation process, the directional features of the spatial correlation should be examined. Variogram surface images were produced to examine the directional features, and an isotropic feature was found. The variogram model's parameters (nugget, sill and range) were determined for this model, as presented in Figure 4. Soil depth data were found to fit well with the spherical model, producing a well-structured semi-variogram with small nugget effects (Nugget = 0.28). The Nugget/Sill ratio for the model was a relatively low 2.19%, indicating that the model was less influenced by random factors (Matheron 1963; Webster and Oliver 1992) and had a strong spatial dependency in these samples. The semi-variogram range was 3.3 km, which showed that within 3.3 km, sampling sites were well autocorrelated. The semi-variogram range was short relatively in such a large grassland ecosystem, where the spatial heterogeneity is stronger than in locations with frequent human activity, such as urban parks and recreational areas, where heterogeneous soil attributes had a relatively short range of 83–133 m (Dao *et al.* 2012). In the study, the relatively short ranges in the semi-variogram compared with the size of the study area showed that the sampling density was not adequate to reveal the soil spatial structures, and denser sampling needs to be carried out in the further investigation.

Cross-validation

Cross-validation can be used to evaluate the effectiveness of the geostatistical model with measurements from the field site. However, these tests cannot detect bias in sampling or analysis. In this study, a good linear relationship between the actual and estimated data sets was obtained. Cross-validation showed a root mean square standardized error of the estimated response variable is 0.93 (the variogram model is optimal when it closed to 1 (Garrigues *et al.* 2006) and a mean standardized error of 0.01 (optimal when close to 0).

Discussion

Spatial distribution of soil depth

A spatial distribution map of soil depth in the grassland was produced using OK (Figure 5). The fitted parameters for the spherical variogram model were used in the interpolation process to quantitatively reveal spatial variability (Webster and Oliver 1992; Burgos *et al.* 2006).

In the spatial distribution map of soil depth, approximately 1% of the area displayed relatively low values of soil depth (15–20 cm), 15% of the area had a range of 20–35 cm, 43% of the area had a range of 35–50 cm, 34% of the area displayed relatively high values (50–65 cm), and 4% of the area had the soil with a range of 65–80 cm, only 3% of the highest value. From these observations, it was clear that the soil depth in the study area ranged predominately from 35–65 cm (approximately 77% of the total area). The relatively deep soils indicate these areas are potentially suitable for the establishment of pastures. However, it is worth noting that

Table 1 Summary statistics for soil depth extracted from ground penetrating radar (GPR) data (n = 121, unit in cm)

Min.	25%	Median	Mean	75%	95%	Max.	Skewness	Kurtosis	SD.
15	30	43	48	57	100	147	1.63	3.31	25.15

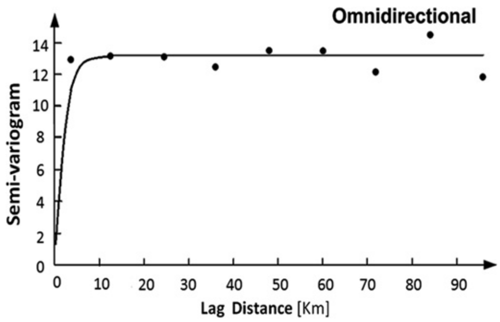

Figure 4 Spherical variogram model of soil depth (Nugget = 0.28, Sill = 12.739, Range = 3.3).

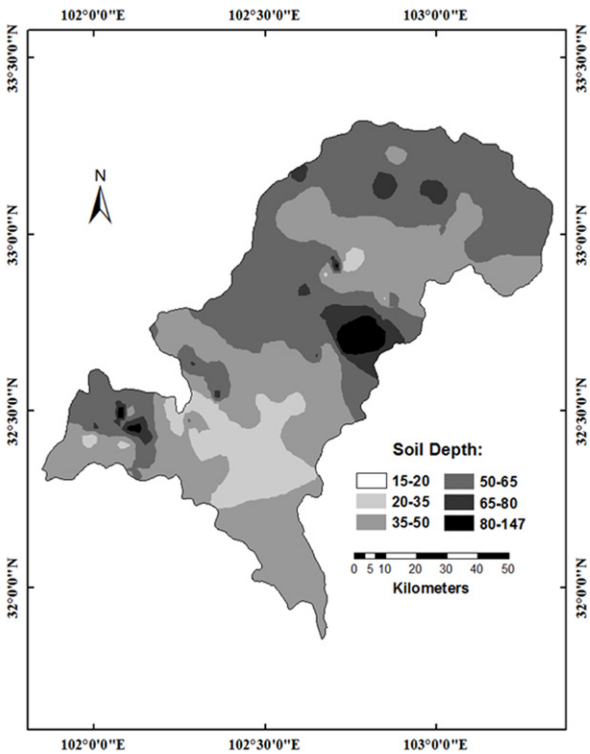

Figure 5 Spatial distribution of soil depth values in Hongyuan, Sichuan, China.

most of the sampling sites were located in flat areas with a slope less than 12°, which could retain more water and nutrients and may have contributed to the higher values observed for soil depth in this area.

Data from previous investigations conducted in the 1980s, measured by profile and location recorded, were used for comparative purposes (Table 2), revealing similar results to the data derived from the spatial distribution map in the current study. However, the ranges of soil depth reported in the present study were lower than the 1980s observations, especially at two locations (Waqie and Sedi village) at which the maximum values exceeded 100 cm in 1980s and have since showed a sharp decrease. Through interviewing experts and working in the field, it emerged that almost all the 1980s sampling sites in the Waqie and Sedi villages were located in the centers of wetlands. Over the years, it is possible that soil was deposited and accumulated in these lower areas, accounting for the greater soil depth values. In contrast, the sampling sites in the current project were predominately located towards the edge of the wetland. Furthermore, the sampling sites in the 1980s study did not use GPS but instead used an old geographic name for identification, making precise spatial comparisons difficult. The average soil depth of the current study was lower than that in the 1980s, which may be the result of drought and geological changes that have occurred over the past 30 years.

The spatial distribution map combined with data from the 1980s survey demonstrated distinct regimes of soil depth, from south to north. The landscape in Hongyuan County has geographical features that range from mountain plateau to hummocky plateau, formed by the uplifting of the Tibetan Plateau and attributable to the activities of glaciers, rivers, and vegetation over time. Due to these diverse geological histories, the spatial distribution of soil depth exhibits an irregular pattern across the study region. According to previous field investigations, the diversity of local micro-topography (Dietrich *et al.* 1995) and hydrogeology (Moore *et al.* 1993) exert significant influences on the spatial variability of soil depth in the study area.Micro-

Table 2 Comparison between soil depth (cm) for the special distribution map in current study and the 1980s investigation

	The 1980s investigation (recorded point)			The special distribution map in current study (same point in special distribution map)		
Village	Minimum	Maximum	Average	Minimum	Maximum	Average
Anqu	16	82	51	32	52	41
Longri	30	88	62	16	74	36
Sedi	43	133	88	40	55	50
Shuajinsi	33	89	60	40	44	43
Waqie	24	100	64	15	78	36

topography in the region was mainly affected by soil production from the underlying bedrock and the divergence of diffusive soil transport. Regional hydrogeology affected the spatial variability of soil depth through activity from the river system. In this study, the relatively thick soils were mainly distributed over colluviums and flood plains. The spatial variability of soil depth and humus content were also affected by the underlying regional geology (parent rock, texture and geomorphology), climate, vegetation and other biotic factors such as anthropogenic and biodynamic impacts (Riha *et al.*1986; Bernier *et al.* 1993; Bernier and Ponge 1994; Ponge 2003; Johnson *et al.* 2005; Aubert *et al.* 2006; Ponge *et al.* 2011; Crouvi *et al.* 2013).

The spatial distribution map clearly illustrated patterns in soil depth, with relatively deep soil in the north, northeast, southwest and relatively shallow soil in the south and northeast of the study area. The greater soil depth values in the north, northeast and southwest correlated to the diversity of local hydrogeology and micro-topography in that region, as well as the distribution of river systems, which caused a thicker soil layer. In the southern study area, the thick soils are most likely a result of large areas of forest and bush laying fallow. This difference in depths confirmed that the distribution of river systems and degree of vegetation cover had a positive influence on soil depth (and *vice versa*) (Delgado *et al.* 2000; Tanaka *et al.* 2009). In the northeastern study area, there is a lower water table, and the subsequent reduced vegetation cover and additional intense farming could have contributed to the shallower soils. Finally, our analysis showed that a large area of swamp and wetland in the north and a region with dense forest in the southwest of Hongyuan County are unsuitable areas for establishing pastures with respect to their soil depths.

Conclusions

Values of the spatial distribution soil depth in Hongyuan County on the Qinghai Tibet Plateau were determined using GPR. Validation results showed that GPR measurements were highly correlated with ground-truthed ruler measurements, and demonstrated that GPR is a suitable technique for measuring soil depth. An interpolated spatial distribution map of soil depth in Hongyuan County was produced with the aid of OK. This procedure demonstrated the high accuracy and non-destructive features of GPR, providing a more systematic and fully spatial distribution map of soil depth than the previous grassland soil survey done in the 1980s.

To create even more accurate maps of soil depth, greater numbers of samples need to be measured in areas where slopes are greater than 12°. Additionally, the proposed GPR technique should be combined with conventional soil depth measurement methods (such as the profile and rod methods) in GPR abnormal signal places.

These results also provide useful data that can help inform sustainable and productive pasture creation and management in the future. For example, in the future, more new pastures should be established in the north, east and southwest of Hongyuan County because of the health of the soil profiles.

Mapping the distribution of soil depth with the aid of GPR and GIS provides useful information for creating soil policy aimed at promoting sustainable agriculture and responsible management of grassland ecosystems.

Acknowledgments

This study was funded by “The technology research and demonstration of high quality forage production in Sichuan pastoral area” (Project No. 201003023) and China Agriculture Research System (Project No. CARS-35-16).

References

Aubert M, Margerie P, Ernoult A, Decaëns T, Bureau F (2006) Variability and heterogeneity of humus forms at stand level: comparison between pure beech and mixed beech-hornbeam forest. *Ann Forest Sci* 63: 177–188.

Bathurst JC, Moretti G, El-Hames A, Beguería S, García-Ruiz JM (2007) Modelling the impact of forest loss on shallow landslide sediment yield, Ijuez river catchment, Spanish Pyrenees. *Hydrol Earth Syst Sci* 11: 569–583.

Beaver WL, Wasserman K, Whipp BJ (1985) Improved detection of lactate threshold during exercise using a log-log transformation. *J Appl Physiol* 59: 1936–1940.

Bernier N, Ponge J-F (1994) Humus form dynamics during the sylvogenetic cycle in a mountain spruce forest. *Soil Biol Biochem* 26: 183–220.

Bernier N, Ponge J-F, André J (1993) Comparative study of soil organic layers in two bilberry-spruce forest stands (Vaccinio). Relation to Forest Dynamics. *Geoderma* 59: 89–108.

Burgos P, Madejón E, Pérez-de-Mora A, Cabrera F (2006) Spatial variability of the chemical characteristics of a trace-element-contaminated soil before and after remediation. *Geoderma* 130: 157–175.

Cerdà A, García-Fayos P (1997) The influence of slope angle on sediment, water and seed losses on badland landscapes. *Geomorphology* 18: 77–90.

Chanzy A, Tarussov A, Bonn F, Judge A (1996) Soil water content determination using a digital ground-penetrating radar. *Soil Sci Soc Am J* 60: 1318–1326.

Chareyre B, Villard P (2005) Dynamic spar elements and discrete element methods in two dimensions for the modeling of soil-inclusion problems. *J Eng Mech* 131: 689–698.

Chartin C, Bourennane H, Salvador-Blanes S, Hinschberger F, Macaire J-J (2011) Classification and mapping of anthropogenic landforms on cultivated hillslopes using DEMs and soil thickness data-Example from the SW Parisian Basin, France. *Geomorphology* 135: 8–20.

Craig RF (1978) *Soil Mechanics*. Wiley, New York, 1–458.

Crouvi O, Pelletier JD, Rasmussen C (2013) Predicting the thickness and aeolian fraction of soils in upland watersheds of the Mojave Desert. *Geoderma* 195: 94–110.

Cundall PA, Strack OD (1979) A discrete numerical model for granular assemblies. *Geotechnique* 29: 47–65.

Daniels DJ (2004) *Ground Penetrating Radar*. Institution of Electrical Engineers, London, 1–752.

Dao L, Morrison L, Zhang C (2012) Bonfires as a potential source of metal pollutants in urban soils, Galway, Ireland. *Appl Geochem* 27: 930–935.

Davis J, Annan A (1989) Ground-Penetrating Radar for high-resolution mapping of soil and rock stratigraphy. *Geophys Prospect* 37: 531–551.

Delgado J, Lopez Casado C, Estevez A, Giner J, Cuenca A, Molina S (2000) Mapping soft soils in the Segura river valley (SE Spain): a case study of microtremors as an exploration tool. *J Appl Geophys* 45: 19–32.

Dietrich WE, Reiss R, Hsu ML, Montgomery DR (1995) A process-based model for colluvial soil depth and shallow landsliding using digital elevation data. *Hydrol Process* 9: 383–400.

Fuhlendorf SD, Smeins FE (1998) The influence of soil depth on plant species response to grazing within a semi-arid savanna. *Plant Ecol* 138: 89–96.

Galagedara L, Parkin G, Redman J, Von Bertoldi P, Endres A (2005) Field studies of the GPR ground wave method for estimating soil water content during irrigation and drainage. *J Hydrol* 301: 182–197.

Garrigues S, Allard D, Baret F, Weiss M (2006) Quantifying spatial heterogeneity at the landscape scale using variogram models. *Remote Sens Environ* 103: 81–96.

Gerber R, Felix Henningsen P, Behrens T, Scholten T (2010) Applicability of ground-penetrating radar as a tool for non-destructive soil depth mapping on Pleistocene periglacial slope deposits. *J Plant Nutr Soil Sci* 173: 173–184.

Gessler PE, Chadwick OA, Chamran F, Althouse L, Holmes K (2000) Modeling soil-landscape and ecosystem properties using terrain attributes. *Soil Sci Soc Am J* 64: 2046–2056.

Grote K, Hubbard S, Rubin Y (2003) Field-scale estimation of volumetric water content using ground-penetrating radar ground wave techniques. *Water Resour Res* 39: 177–178.

Güneralp İ, Rhoads BL (2009) Empirical analysis of the planform curvature-migration relation of meandering rivers. *Water Resour Res* 45: 233–236.

Helsel DR (1987) Advantages of nonparametric procedures for analysis of water quality data. *Hydrolog Sci J* 32: 179–190.

Hong Y, Hong B, Lin Q *et al.* (2003) Correlation between Indian Ocean summer monsoon and North Atlantic climate during the Holocene. *Earth Plant Sc Lett* 211: 371–380.

Hubbard S, Grote K, Rubin Y (2002) Mapping the volumetric soil water content of a California vineyard using high-frequency GPR ground wave data. *Lead Edge* 21: 552–559.

Huisman J, Hubbard S, Redman J, Annan A (2003) Measuring soil water content with ground penetrating radar. *Vadose Zone J* 2: 476–491.

Johnson D, Domier J, Johnson D (2005) Animating the biodynamics of soil thickness using process vector analysis: a dynamic denudation approach to soil formation. *Geomorphology* 67: 23–46.

Kreutzmann H (2012) Pastoral practices in High Asia. In: *Advances in Asian Human-Environmental Research, Enclosure and Resettlement in the Eastern Tibetan Plateau: Dilemma of Pastoral Development During the Last Three Decades* (Eds Ning W, Zhaoli Y, Tao L), Springer, Dordrecht, 291–306

Kuriakose SL, Devkota S, Rossiter DG, Jetten VG (2009) Prediction of soil depth using environmental variables in an anthropogenic landscape, a case study in the Western Ghats of Kerala, India. *Catena* 79: 27–38.

Lambot S, Antoine M, Vanclooster M, Slob EC (2006) Effect of soil roughness on the inversion of off-ground monostatic GPR signal for noninvasive quantification of soil properties. *Water Resour Res* 42: 216–224.

Lee KS, Lee GB, Tyler EJ (1988) Thematic mapper and digital elevation modeling of soil characteristics in hilly terrain. *Soil Sci Soc Am J* 52: 1104–1107.

Lin X, Ng T-T (1997) A three-dimensional discrete element model using arrays of ellipsoids. *Geotechnique* 47: 319–329.

Lowe DJ (1985) Application of impulse radar to continuous profiling of tephra-bearing lake sediments and peats: an initial evaluation. *New Zeal J Geol Geop* 28: 667–674.

Matheron G (1963) Principles of geostatistics. *Econ Geol* 58: 1246–1266.

McBratney A, Webster R (1986) Choosing functions for semi-variograms of soil properties and fitting them to sampling estimates. *J Soil Sci* 37: 617–639.

McGrath D, Zhang C (2003) Spatial distribution of soil organic carbon concentrations in grassland of Ireland. *Appl Geochem* 18: 1629–1639.

Meyer MD, North MP, Gray AN, Zald HSJ (2007) Influence of soil thickness on stand characteristics in a Sierra Nevada mixed-conifer forest. *Plant Soil* 294: 113–123.

Minasny B, McBratney AB (1999) A rudimentary mechanistic model for soil production and landscape development. *Geoderma* 90: 3–21.

Minet J, Lambot S, Slob EC, Vanclooster M (2010) Soil surface water content estimation by full-waveform GPR signal inversion in the presence of thin layers. *IEEE T Geosci Remote* 48: 1138–1150.

Moore ID, Gessler PE, Nielsen GA, Peterson GA (1993) Soil attribute prediction using terrain analysis. *Soil Sci Soc Am J* 57: 443–452.

Moris JR (1988) *Oxfam's Kenya Restocking Projects*. Overseas Development Institute, London, 1–20.

Neal A (2004) Ground-penetrating radar and its use in sedimentology: principles, problems and progress. *Earth-Sci Rev* 66: 261–330.

Oliver MA, Webster R (1986) Semi-variograms for modelling the spatial pattern of landform and soil properties. *Earth Surf Proc Land* 11: 491–504.

Pachepsky YA, Timlin DJ, Rawls WJ (2001) Soil water retention as related to topographic variables. *Soil Sci Soc Am J* 65: 1787–1795.

Pennock D, De Jong E (1987) The influence of slope curvature on soil erosion and deposition in hummock terrain. *Soil Sci* 144: 209–217.

Phillips JD (2010) The convenient fiction of steady-state soil thickness. *Geoderma* 156: 389–398.

Ponge J-F (2003) Humus forms in terrestrial ecosystems: a framework to biodiversity. *Soil Biol Biochem* 35: 935–945.

Ponge J-F, Jabiol B, Gégout J-C (2011) Geology and climate conditions affect more humus forms than forest canopies at large scale in temperate forests. *Soil Biol Biochem* 162: 187–195.

Previati M, Godio A, Ferraris S (2011) Validation of spatial variability of snowpack thickness and density obtained with GPR and TDR methods. *J Appl Geophys* 75: 284–293.

Prior J (1994) *Pastoral Development Planning*. Oxfam, Oxford, 1–150.

Qin D, Xie Z, Tang S (1984) *Hongyuan Soil*. Sichuan Science and Technology Publishing House, Chengdu, 1–113.

Rhoton FE, Lindbo DL (1997) A soil depth approach to soil quality assessment. *J Soil Water Conserv* 52: 66–72.

Riha SJ, James BR, Senesac GP, Pallant E (1986) Spatial variability of soil pH and organic matter in forest plantations. *Soil Sci Soc Am J* 50: 1347–1352.

Sandford S (1983) Management of pastoral development in the Third World. *Poulation Develop Rev* 2: 157–158.

Schmalz B, Lennartz B (2002) Analyses of soil water content variations and GPR attribute distributions. *J Hydrol* 267: 217–226.

Shih S, Doolittle J (1984) Using radar to investigate organic soil thickness in the Florida Everglades. *Soil Sci Soc Am J* 48: 651–656.

Sucre EB, Tuttle JW, Fox TR (2011) The use of Ground-Penetrating Radar to accurately estimate soil depth in Rocky forest soils. *Forest Sci* 57: 59–66.

Tanaka S, Tachibe S, Wasli MEB *et al.* (2009) Soil characteristics under cash crop farming in upland areas of Sarawak, Malaysia. *Agr Ecosyst Environ* 129: 293–301.

Wang J, Endreny TA, Hassett JM (2006) Power function decay of hydraulic conductivity for a Topmodel-based infiltration routine. *Hydrol Process* 20: 3825–3834.

Webster R, Oliver MA (1992) Sample adequately to estimate variograms of soil properties. *J Soil Sci* 43: 177–192.

Weijun F, Huber T, Chaosheng Z (2010) Spatial variation of soil nutrients in a dairy farm and its implications for site-specific fertilizer application. *Soil Tillage Res* 106: 185–193.

Whelan KRT, Smith TJ, Cahoon DR, Lynch JC, Anderson GH (2005) Groundwater control of mangrove surface elevation: shrink and swell varies with soil depth. *Estuar Coast* 28: 833–843.

Yamakawa Y, Kosugi KI, Masaoka N, Sumida J, Tani M, Mizuyama T (2012) Combined geophysical methods for detecting soil thickness distribution on a weathered granitic hillslope. *Geomorphology* 145: 56–69.

Yamamoto S, Kawamura K, Seki O, Meyers PA, Zheng Y, Zhou W (2010) Paleoenvironmental significance of compound-specific δ13 C variations in n-alkanes in the Hongyuan peat sequence from southwest China over the last 13ka. *Org Geochem* 41: 491–497.